

The influence of the enhanced vector meson sector on the properties of the matter of neutron stars.

Ilona Bednarek, Ryszard Manka,* and Monika Pienkos
*Department of Astrophysics and Cosmology, Institute of Physics,
University of Silesia, Uniwersytecka 4, 40-007 Katowice, Poland*

(Dated: February 27, 2022)

This paper gives an overview of the model of a neutron star with non-zero strangeness constructed within the framework of the nonlinear realization of the chiral $SU(3)_L \times SU(3)_R$ symmetry. The emphasis is put on the physical properties of the matter of a neutron star. The obtained solution is particularly aimed at the problem of the construction of a theoretical model of a neutron star matter with hyperons that will give high value of the maximum mass.

PACS numbers: 97.60.Jd, 26.60.Kp, 21.65.Mn, 14.20.Jn

I. INTRODUCTION

The description of the core of a neutron star is modelled on the basis of the equation of state (EoS) of dense asymmetric nuclear matter [1]. The matter density ranges from a few times the saturation density (n_0) to about an order of a magnitude higher at the core of a neutron star and at such densities hyperons are expected to emerge [2]. The purpose of this paper is to study the impact of hyperons on the properties of the matter of neutron stars, and on their structure. In general, analysis of the role of strangeness in nuclear structure in the aspect of multi-strange system is of great importance for both nuclear physics and for astrophysics and leads to a proper understanding of the properties of a hyperon star.

The relativistic approach to the description of nuclear matter developed by Walecka [3] is very successful in describing a variety of the ground state properties of finite nuclei. Although the original Walecka model properly describes the saturation point and the data for finite nuclei, it has been insufficient to properly describe the compression modulus of symmetric nuclear matter at saturation density. The nonlinear self-interactions of the scalar field (the cubic and quartic terms) were added in order to get an acceptable value of the compression modulus [4, 5]. Additionally the inclusion of a quartic vector self-interaction term softens the high density component of the EoS [6]. The estimation of the incompressibility coefficient of symmetric nuclear matter K_0 , which is made on the basis of recent experimental data, points to the range 240 ± 10 MeV [7].

Models that satisfactorily reproduce the saturation properties of symmetric nuclear matter lead to considerable differences in a case in which asymmetry dependence is included [8, 9]. Thus, the proper model of the matter of neutron stars requires taking the effect of neutron-proton asymmetry into consideration. This, in turn, leads to the inclusion of the isovector meson ρ . The standard version of the introduction of the ρ meson field is of a minimal

type without any nonlinearities. This case has been further enlarged by the nonlinear mixed isoscalar-isovector couplings, which modify the density dependence of the ρ mean field and the symmetry energy [10–12]. The analysis of the nonlinear models should include results obtained for the relativistic FSUGold parametrisation [13].

A theoretical description of strangeness-rich nuclear matter requires the extension of the model to the full octet of baryons and additional meson fields were introduced to reproduce the hyperon–hyperon interaction. The model that is considered is constructed on the basis of the hadronic $SU(3)$ theory, which naturally includes nonlinear scalar and vector interaction terms. The characteristic feature of the model is the very special form of the vector meson sector, which permits more accurate description of asymmetric strangeness-rich neutron star matter [14]. The primary goal of this paper is to maximize the understanding of the influence of the nonlinear vector meson couplings on the form of the EoS and through this on a neutron star structure.

The calculated EoS for the matter of neutron stars in the case when hyperons are included have shown considerable stiffening for higher densities. Having obtained the EoS the analysis of the maximum achievable neutron star mass for a given class of models can be performed. Observational results limit the value of a neutron star mass and thereby put constraints on the EoS of high density nuclear matter. Recent observations point to the existence of a high maximum neutron star mass [15, 16], what is inconsistent with theoretical models that involve hyperons.

II. THE MODEL

Recent observations of the binary millisecond pulsar J1614-2230 [15] and J0348+0432 [16] have led to an estimation of the neutron star mass within the range respectively $(1.97 \pm 0.04)M_\odot$ and $(2.01 \pm 0.04)M_\odot$. This places the maximum neutron star mass at rather high values and rules out most of the EoSs with hyperons as models that involve exotic particles predict maximum neutron star masses well below the stated value. There is a need

* Retired

to analyse whether it is possible to construct an EoS of neutron star matter that gives adequately high maximum mass despite including hyperons. In this paper a description of nuclear matter based on an effective model constructed within the framework of the nonlinear realization of the chiral $SU(3)_L \times SU(3)_R$ symmetry. Details can be found in the papers by Papazoglou et al. [17, 18].

Baryons and mesons constitute the basic degrees of freedom of the model, and consequently the Lagrangian density function \mathcal{L} splits into parts that are adequate to describe baryon \mathcal{L}_B and meson \mathcal{L}_M sectors supplemented

by the term that represents baryon–meson interactions \mathcal{L}_{int} , and takes the form $\mathcal{L} = \mathcal{L}_B + \mathcal{L}_M + \mathcal{L}_{int}$.

The meson sector of the considered model includes spin zero and spin one meson states. Nonets of different meson types, spin zero (scalar) and spin one (vector), can be written as the sum of the singlet and octet matrixes $\mathcal{M} = \mathcal{M}_{sin} + \mathcal{M}_{oct}$. Under the assumption of SU(3) symmetry, a very general form of the interaction Lagrangian \mathcal{L}_{int} includes a mixture of the symmetric (D -type) and antisymmetric (F -type) couplings and the S -type coupling that denotes the meson singlet state interaction

$$\begin{aligned} \mathcal{L}_{int} &= -\sqrt{2}g_8^M(\alpha_M[\bar{\mathcal{B}}\mathcal{B}\mathcal{M}]_F + (1 - \alpha_M)[\bar{\mathcal{B}}\mathcal{B}\mathcal{M}]_D) - g_1^M \frac{1}{\sqrt{3}}[\bar{\mathcal{B}}\mathcal{B}\mathcal{M}]_{sin} = \\ &= -\sqrt{2}g_8^M[\alpha_M(Tr(\bar{\mathcal{B}}\mathcal{M}_{oct}\mathcal{B}) - Tr(\bar{\mathcal{B}}\mathcal{B}\mathcal{M}_{oct})) + (1 - \alpha_M)(Tr(\bar{\mathcal{B}}\mathcal{M}_{oct}\mathcal{B}) + Tr(\bar{\mathcal{B}}\mathcal{B}\mathcal{M}_{oct}))] - \\ &- g_1^M \frac{1}{\sqrt{3}}Tr(\bar{\mathcal{B}}\mathcal{B})Tr(\mathcal{M}_{sin}), \end{aligned} \quad (1)$$

where the explicitly given baryon matrix \mathcal{B} has the form

$$\mathcal{B} = \begin{pmatrix} \frac{1}{\sqrt{6}}\Lambda + \frac{1}{\sqrt{2}}\Sigma^0 & \Sigma^+ & p \\ \Sigma^- & \frac{1}{\sqrt{6}}\Lambda - \frac{1}{\sqrt{2}}\Sigma^0 & n \\ \Xi^- & \Xi^0 & -\frac{2}{\sqrt{6}}\Lambda \end{pmatrix}. \quad (2)$$

Generally, the baryon–meson interaction is characterised by the following coupling constants: the octet g_8^M and singlet g_1^M coupling constant, the parameter α_M , which stands for the $F/(F + D)$ ratio, and a mixing angle θ_M that relates the physical meson fields to the pure octet and singlet states. The index \mathcal{M} concerns the interaction of baryons with scalar ($\mathcal{M} = S$) and vector ($\mathcal{M} = V$) mesons (pseudoscalar and axial vector mesons, which have a vanishing expectation value at the mean field level, are not considered in this model). In the case of the scalar meson sector baryon masses are generated by the vacuum expectation value that is attained by two scalar meson fields and the parameters g_1^S, g_8^S , and α_S have been chosen to fit the experimental values of the baryon-octet masses [17, 18]. Considering the vector meson sector of this model the octet matrix

$$V_{oct} = \begin{pmatrix} \frac{v_8}{\sqrt{6}} + \frac{\rho^0}{\sqrt{2}} & \rho^+ & K^{*+} \\ \rho^- & \frac{v_8}{\sqrt{6}} - \frac{\rho^0}{\sqrt{2}} & K^{*0} \\ K^{*-} & \bar{K}^{*0} & -\frac{2v_8}{\sqrt{6}} \end{pmatrix} \quad (3)$$

supplemented with the singlet state

$$V_{sin} = \frac{1}{\sqrt{3}}diag(v_0, v_0, v_0)$$

comprises the vector meson nonet. The combinations of the unphysical SU(3) singlet (v_0) and octet (v_8) states

produce the physical ω and ϕ mesons

$$\begin{aligned} \phi &= v_8 \cos \theta_V - v_0 \sin \theta_V, \\ \omega &= v_8 \sin \theta_V + v_0 \cos \theta_V. \end{aligned} \quad (4)$$

The ϕ meson taken as pure $\bar{s}s$ state leads to the ideal mixing with $\theta_V \approx 35.3^\circ$. If the determination of the baryon–vector meson couplings bases on the assumption that nucleons do not couple to the $\bar{s}s$ meson, then $g_1^V = \sqrt{6}g_8^V$. In the limit $\alpha_V = 0$ (only the F -type coupling remains), the coupling constants are related to the additive quark model and the vector meson coupling constants are given by the following relations:

$$\begin{aligned} g_{\Lambda\omega} &= g_{\Sigma\omega} = 2g_{\Xi\omega} = \frac{2}{3}g_{N\omega} = 2g_8^V, \\ g_{\Lambda\phi} &= g_{\Sigma\phi} = \frac{g_{\Xi\phi}}{2} = \frac{\sqrt{2}}{3}g_{N\omega}. \end{aligned} \quad (5)$$

The high density limit of the EoS of dense matter in neutron star interiors is dominated by the contribution that come from the baryon number density, which justifies the construction of a model that includes a broad spectrum of mixed vector meson couplings. The extended vector meson sector, which stems from the SU(3) invariants, can be written in the following form

$$\mathcal{L}_V = \frac{1}{4}c(Tr(VV))^2 + \frac{1}{2}dTr((VV)^2) + \frac{1}{16}f(Tr(V))^4,$$

where V represents the matrix of the vector meson fields, and c, d, f are the general coefficients that have been determined by assuming that in the case of a neutron star with zero strangeness, the model described by the TM1 parameter set [6] is recovered. This assumption leads to the Lagrangian function, which embodies contributions from the baryon and meson sectors supplemented by the parts that describe the baryon and meson interactions

$$\begin{aligned} \mathcal{L} = & \sum_B \bar{\psi}_B (i\gamma^\mu D_\mu - m_{eff,B}) \psi_B + \frac{1}{2} \partial^\mu \sigma \partial_\mu \sigma - \frac{1}{2} m_\sigma^2 \sigma^2 - \frac{1}{3} g_3 \sigma^3 - \frac{1}{4} g_4 \sigma^4 + \frac{1}{2} \partial^\mu \sigma^* \partial_\mu \sigma^* - \frac{1}{2} m_{\sigma^*}^2 \sigma^{*2} + \\ & + \frac{1}{2} m_\omega^2 (\omega^\mu \omega_\mu) + \frac{1}{2} m_\rho^2 (\rho^{\mu a} \rho_\mu^a) + \frac{1}{2} m_\phi^2 (\phi^\mu \phi_\mu) - \frac{1}{4} \Omega^{\mu\nu} \Omega_{\mu\nu} - \frac{1}{4} \mathbf{R}^{\mu\nu} \mathbf{R}_{\mu\nu} - \frac{1}{4} \Phi^{\mu\nu} \Phi_{\mu\nu} + U_{nonl}^{vec}(\omega, \rho, \phi) + \mathcal{L}_l, \end{aligned} \quad (6)$$

where the covariant derivative equals $D_\mu = \partial_\mu + ig_{B\omega}\omega_\mu + ig_{B\phi}\phi_\mu + ig_{B\rho}\mathbf{I}_B\rho_\mu$, \mathbf{I}_B denotes isospin of baryon B . The baryon effective mass is defined as follows $m_{eff,B} = m_B - g_{B\sigma}\sigma - g_{B\sigma^*}\sigma^*$ while $\Omega_{\mu\nu}$, $\mathbf{R}_{\mu\nu}$, and $\Phi_{\mu\nu}$ are the field tensors of the ω , ρ , and ϕ mesons. A proper description of hyperon-hyperon interaction requires the presence of hidden strangeness mesons: scalar (σ^*) and vector (ϕ). The Lagrangian function (6) describes the β -equilibrated neutron star matter; thus there is also a need to consider the Lagrangian of free leptons \mathcal{L}_l

$$\mathcal{L}_l = \sum_{l=e,\mu} \bar{\psi}_l (i\gamma^\mu \partial_\mu - m_l) \psi_l, \quad (7)$$

All nonlinear vector meson couplings that occur in this model have been brought together in the form of a vector potential

$$\begin{aligned} U_{nonl}^{vec}(\omega, \rho, \phi) = & \frac{1}{4} c_3 (\omega^\mu \omega_\mu)^2 + \frac{1}{4} c_3 (\rho^{\mu a} \rho_\mu^a)^2 + \frac{1}{8} c_3 (\phi^\mu \phi_\mu)^2 + \Lambda_V (g_{N\omega} g_{N\rho})^2 (\omega^\mu \omega_\mu) (\rho^{\mu a} \rho_\mu^a) + \\ & + \frac{1}{2} \left(\frac{3}{2} c_3 - \Lambda_V (g_{N\omega} g_{N\rho})^2 \right) (\phi^\mu \phi_\mu) (\omega^\mu \omega_\mu + \rho^{\mu a} \rho_\mu^a) + \frac{1}{4} \Lambda_V (g_{N\omega} g_{N\rho})^2 (\phi^\mu \phi_\mu)^2. \end{aligned} \quad (8)$$

The description of dense, hyperon-rich nuclear matter given by the Lagrangian (6) in the case of non-strange matter is reduced to the standard TM1 model with an extended isovector sector. This extension refers to the presence of the $\omega - \rho$ meson coupling and enables modification of the high density limit of the symmetry energy. The strength of this coupling is characterised by parameter Λ_V . For each value of parameter Λ_V , the parameter $g_{N\rho}$ has to be adjusted to reproduce the symmetry energy $E_{sym} = 25.68$ MeV at $k_F = 1.15$ fm $^{-1}$ [19].

III. THE EQUATION OF STATE

The mean field approach has been adopted to calculate the EoS. In this approximation, meson fields are separated

into classical mean field values: $s_0, s_0^*, w_0, r_0, f_0$ and quantum fluctuations, which are neglected in the ground state:

$$\begin{aligned} \sigma &= \tilde{\sigma} + s_0, & \sigma^* &= \tilde{\sigma}^* + s_0^* \\ \omega_\mu &= \tilde{\omega}_\mu + w_0, & w_0 &\equiv \langle \omega_\mu \rangle \delta_{0\mu} = \langle \omega_0 \rangle \\ \rho_\mu^a &= \tilde{\rho}_\mu^a + r_0, & r_0 &\equiv \langle \rho_\mu^a \rangle \delta_{0\mu} \delta^{3a} = \langle \rho_0 \rangle \\ \phi_\mu &= \tilde{\phi}_\mu + f_0, & f_0 &\equiv \langle \phi_\mu \rangle \delta_{0\mu} = \langle \phi_0 \rangle \end{aligned}$$

The preferable attribute of the considered model is its very diverse vector meson sector, which allows one to study the relevance of different vector meson couplings for the form of the EoS. The Lagrangian function (6) makes it possible to calculate the equations of motion from the corresponding Euler-Lagrange equations. The obtained results, written in the mean field approximation, take the form:

$$m_\sigma^2 s_0 = -g_3 s_0^3 - g_4 s_0^4 + \sum_B g_{B\sigma} \frac{2J_B + 1}{2\pi^2} \int_0^{k_{F,B}} \frac{m_{eff,B}(s_0, s_0^*) k^2}{\sqrt{(k^2 + m_{eff,B}^2(s_0, s_0^*))}} \quad (9)$$

$$m_{\sigma^*}^2 s_0^* = \sum_B g_{B\sigma^*} \frac{2J_B + 1}{2\pi^2} \int_0^{k_{F,B}} \frac{m_{eff,B}(s_0, s_0^*) k^2}{\sqrt{(k^2 + m_{eff,B}^2(s_0, s_0^*))}} \quad (10)$$

$$m_{eff,\omega}^2 w_0 - 2c_3 w_0^3 = g_{B\omega} \delta_Q n_b, \quad (11)$$

$$m_{eff,\rho}^2 r_0 - 2c_3 r_0^3 = g_{B\rho} \delta_3 n_b, \quad (12)$$

$$m_{eff,\phi}^2 f_0 - (c_3 + 2\Lambda_V (g_{B\omega} g_{B\rho})^2) f_0^3 = g_{B\phi} \delta_S n_b, \quad (13)$$

$$(i\gamma^\mu \partial_\mu - m_{eff,B} - g_{B\omega}(1-x_B)\gamma^0 w_0 - g_{B\rho} I_{3B} \gamma^0 \tau^3 r_0 - g_{B\phi} x_B \gamma^0 f_0) \psi_B = 0, \quad (14)$$

where J_B and I_{3B} denote the spin and isospin projection of baryon B , $m_{eff,i}$, ($i = \omega, \rho, \phi$) are effective masses assigned to vector meson fields:

$$m_{eff,\omega}^2 = m_\omega^2 + 2\Lambda_V (g_{B\omega} g_{B\rho})^2 r_0^2 + \left(\frac{3}{2}c_3 - \Lambda_V (g_{B\omega} g_{B\rho})^2\right) f_0^2 + 3c_3 w_0^2 \quad (15)$$

$$m_{eff,\rho}^2 = m_\rho^2 + 2\Lambda_V (g_{B\omega} g_{B\rho})^2 w_0^2 + \left(\frac{3}{2}c_3 - \Lambda_V (g_{B\omega} g_{B\rho})^2\right) f_0^2 + 3c_3 r_0^2 \quad (16)$$

$$m_{eff,\phi}^2 = m_\phi^2 + \left(\frac{3}{2}c_3 - \Lambda_V (g_{B\omega} g_{B\rho})^2\right) (w_0^2 + r_0^2) + f_0^2 \left(\frac{3}{4}c_3 + \Lambda_V (g_{B\omega} g_{B\rho})^2\right). \quad (17)$$

Analysis of the equations of motion raises the issue of the medium effects on the hadronic matter properties that lead to the problem of the reduced effective baryon masses $m_{eff,B}$. Considering the case in which nucleon mass depends only on non-strange condensate and referring to the Walecka model, the relation for the effective baryon masses in the medium in the relativistic mean field description [10] can be formulated as

$$m_{eff,B} = m_{eff,B}(s_0, s_0^*) = m_B - g_{B\sigma} s_0 - g_{B\sigma^*} s_0^* \quad (18)$$

where the terms $g_{B\sigma} s_0$ and $g_{B\sigma^*} s_0^*$ represent the modification of baryon masses due to the medium.

The source terms in equations (11-13) can be expressed by introducing the parameters δ_Q and δ_S , which measure the contributions of strange (x_B) and non-strange quarks:

$$\delta_Q = \sum_B (1-x_B) \frac{n_B}{n_b} \quad (19)$$

$$\delta_3 = \sum_B I_{3B} \frac{n_B}{n_b} \quad (20)$$

$$\delta_S = \sum_B x_B \frac{n_B}{n_b}. \quad (21)$$

Thus, the number density of u and d quarks refers to δ_Q , whereas the number density of strange quarks is given in terms of the parameter δ_S . The parameter δ_3 aims to evaluate the difference between the density of u and d quarks, $n_b = \sum_B n_B$ denotes the total baryon number density. The baryon-vector meson coupling constants determined from the symmetry relations have been summarised in Table I.

The numerical solution of the equations of motion, which depends on the form of the effective vector potential U_{nonl}^{vec} , has been limited to the result with only one single real solution. The demand for the existence of one real solution puts constraints on the value of parameter Λ_V . Such an analysis in the simpler case of symmetric nuclear matter leads to an equation that relates Λ_V and

TABLE I. Baryon-vector meson coupling constants, $g_{B\omega} = (1-x_B)g_{N\omega}$ and x_B counts the contribution of strange quarks, $g_{N\omega} \equiv g_\omega$ and $g_{N\rho} \equiv g_\rho$.

Baryon (B)	x_B	$g_{B\omega}$	$g_{B\phi} = x_B g_{N\omega}$	$g_{B\rho}$
n	0	g_ω	0	g_ρ
p	0	g_ω	0	g_ρ
Λ	$\frac{1}{3}$	$\frac{2}{3}g_\omega$	$-\frac{\sqrt{2}}{3}g_\omega$	0
Σ	$\frac{1}{3}$	$\frac{2}{3}g_\omega$	$-\frac{\sqrt{2}}{3}g_\omega$	$2g_\rho$
Ξ	$\frac{2}{3}$	$\frac{1}{3}g_\omega$	$-2\frac{\sqrt{2}}{3}g_\omega$	g_ρ

TABLE II. The critical value of the parameter $\Lambda_{V,cr}$ calculated for the selected parameterisations and the incompressibility K_0 taken at the saturation density.

Parameter set	c_3	$\Lambda_{V,cr}$	K_0 (MeV)
NL3 [20]	0	-	271
FSUGold [13]	418.39	0.0517	230
TMA [21]	151.59	0.0318	318
TM1* [22]	134.624	0.0215	281.1
TM1 [6]	71.3	0.0156	281.1
TM2 [23]	84.5318	0.0186	343.8

c_3 parameters and enables the critical value of parameter $\Lambda_{V,cr}$ to be estimated

$$-\frac{7}{4}c_3^2 + 4\Lambda_V c_3 (g_\omega g_\rho)^2 - \Lambda_V^2 (g_\omega g_\rho)^4 = 0. \quad (22)$$

The existence of one single real solution is not satisfied for $\Lambda_V > \Lambda_{V,cr}$. The critical value of the parameter $\Lambda_{V,cr}$ calculated for the selected parameterisations are collected in Table II. In order to calculate the energy density and pressure of the nuclear matter, the energy momentum tensor $T_{\mu\nu}$, which is given by the relation

$$T_{\mu\nu} = \frac{\partial \mathcal{L}}{\partial(\partial_\mu \varphi_i)} \partial^\nu \varphi_i - \eta_{\mu\nu} \mathcal{L} \quad (23)$$

has to be used. In equation (23) φ_i denotes the boson and fermion fields. The energy density \mathcal{E} is equal to $\langle T_{00} \rangle$,

whereas the pressure \mathcal{P} is related to the statistical average of the trace of the spatial component T_{ij} of the energy

$$\begin{aligned} \mathcal{E} = & \frac{1}{2}m_\omega^2 w_0^2 + \frac{1}{2}m_\rho^2 r_0^2 + \frac{1}{2}m_\phi^2 f_0^2 + \frac{1}{2}m_\sigma^2 s_0^2 + \frac{1}{3}g_3 s_0^3 + \frac{1}{4}g_4 s_0^4 + \frac{1}{2}m_{\sigma^*}^2 s_0^{*2} + \frac{3}{4}c_3 (w_0^4 + r_0^4) + \\ & + 3\Lambda_V (g_\omega g_\rho)^2 w_0^2 r_0^2 + \frac{3}{2} \left(\frac{3}{2}c_3 - \Lambda_V (g_\omega g_\rho)^2 \right) (w_0^2 + r_0^2) f_0^2 + 3 \left(\frac{1}{8}c_3 + \frac{1}{4}\Lambda_V (g_\omega g_\rho)^2 \right) f_0^4 + \\ & + \sum_B \frac{2}{\pi^2} \int_0^{k_{F,B}} k^2 dk \sqrt{k^2 + m_{eff,B}^2} + \mathcal{E}_L, \end{aligned} \quad (24)$$

$$\begin{aligned} \mathcal{P} = & \frac{1}{2}m_\omega^2 w_0^2 + \frac{1}{2}m_\rho^2 r_0^2 + \frac{1}{2}m_\phi^2 f_0^2 - \frac{1}{2}m_\sigma^2 s_0^2 - \frac{1}{3}g_3 s_0^3 - \frac{1}{4}g_4 s_0^4 - \frac{1}{2}m_{\sigma^*}^2 s_0^{*2} + \frac{1}{4}c_3 (w_0^4 + r_0^4) + \\ & + \Lambda_V (g_\omega g_\rho)^2 w_0^2 r_0^2 + \frac{1}{2} \left(\frac{3}{2}c_3 - \Lambda_V (g_\omega g_\rho)^2 \right) f_0^2 (w_0^2 + r_0^2) + \left(\frac{1}{8}c_3 + \frac{1}{4}\Lambda_V (g_\omega g_\rho)^2 \right) f_0^4 + \\ & + \sum_B \frac{1}{3\pi^2} \int_0^{k_{F,B}} \frac{k^4 dk}{\sqrt{k^2 + m_{eff,B}^2}} + \mathcal{P}_L \end{aligned} \quad (25)$$

where \mathcal{E}_L and \mathcal{P}_L denote the contributions coming from leptons.

IV. COUPLING CONSTANTS

A. Strange baryons

Understanding the nature of interactions between baryons is a decisive factor for the properties of neutron stars. A precise description of baryon interactions in the strange sector of the model is essential for the correct construction of the EoS. However, the incompleteness of the experimental data intensifies the uncertainties that are connected with the evaluation of coupling constants that involve strange baryons. In general, there are very few data available to describe hyperon–nucleon (YN) and hyperon–hyperon (YY) interactions. Hyperon–vector meson coupling constants are taken from the quark model. They are summarised in Table I. In the scalar sector, the scalar couplings $g_{B\sigma}$ of the Λ , Σ and Ξ hyperons require constraining in order to reproduce the estimated values of the potentials felt by a single Λ , Σ and Ξ in the saturated nuclear matter. In the case of Λ hypernuclei there is a considerable amount of data on binding energies and single particle levels allowing the identification of the potential felt by a single Λ in nuclear matter in the range $U_\Lambda^{(N)} \approx 27 - 30$ MeV [24, 25]. Considering the Ξ hypernuclei current knowledge about the interaction of Ξ hyperons with nuclei is very limited. Dover and Gal [26] based on early emulsion data indicated an attractive Ξ -nucleus potential of the order of 21-24 MeV. This result agrees with theoretical predic-

momentum tensor. Calculations done for the considered model lead to the following explicit formulas for the energy density and pressure:

tions for Ξ in nuclear matter obtained in the model D of the Nijmegen group [27]. However, the missing-mass spectra of a double-charge exchange reaction (K^- , K^+) on a ^{12}C target have suggested the Ξ well depth of 14-16 MeV [28, 29]. Analysis of the experimental data indicate a repulsive Σ -nucleus potential [30], with a substantial isospin dependence [31]. In the case of YY interactions, the only sources of information are the double-strange hypernuclear systems. Several events have been identified that suggest an attractive $\Lambda\Lambda$ interaction. The most promising results, known as the NAGARA event [32] with the ${}^6_{\Lambda\Lambda}\text{He}$ hypernucleus, indicate that the $\Lambda\Lambda$ interaction is weakly attractive. The estimated value of the $U_\Lambda^{(\Lambda)}$ potential at the level of 5 MeV permits a parameter set which reproduces this weaker $\Lambda\Lambda$ interaction to be estimated [33].

The potential that describe hyperon–nucleon and hyperon–hyperon interaction can be written in the form that involves both the scalar and vector coupling constants

$$\begin{aligned} U_Y^{(B)} = & g_{Y\sigma} s_0 - g_{Y\omega} w_0 + g_{Y\sigma^*} s_0^* - g_{Y\phi} f_0 = \\ = & m_Y - m_{eff,Y}(s_0, s_0^*) - (g_{Y\omega} w_0 + g_{Y\phi} f_0), \end{aligned} \quad (26)$$

where $m_{eff,Y}(s_0, s_0^*)$ is the effective mass and Y stands for the Λ , Σ and Ξ hyperons. For the determination of the $g_{\Lambda\sigma}$, $g_{\Sigma\sigma}$ and $g_{\Xi\sigma}$ coupling constants, the following values of the potentials were used

$$U_\Lambda^{(N)} = -28\text{MeV}, \quad U_\Sigma^{(N)} = +30\text{MeV}, \quad U_\Xi^{(N)} = -18\text{MeV}. \quad (27)$$

In general the coupling constants $g_{Y\sigma}$ can be decomposed into two parts $g_{Y\sigma} = g_\sigma x_{Y\sigma}$, where $x_{Y\sigma}$ depends on the value of potential $U_Y^{(N)}$. The coupling of hyperons to the

TABLE III. The scalar coupling constants.

$g_{\Lambda\sigma}$	$g_{\Xi\sigma}$	$g_{\Sigma\sigma}$	$g_{\Lambda\sigma^*}$	$g_{\Xi\sigma^*}$	$g_{\Sigma\sigma^*}$
6.169	3.201	4.476	5.262	11.623	5.626

TABLE IV. Scalar coupling constants calculated for chosen values of the potentials $U_{\Sigma}^{(N)}$ and $U_{\Xi}^{(N)}$.

$U_{\Sigma}^{(N)}$ (MeV)	$U_{\Xi}^{(N)}$ (MeV)	$g_{\Lambda\sigma}$	$g_{\Xi\sigma}$	$g_{\Sigma\sigma}$	$g_{\Xi\sigma^*}$	$g_{\Sigma\sigma^*}$
+30	-14	6.169	3.084	4.476	5.626	11.474
+30	-18	6.169	3.201	4.476	5.482	11.372
+20	-18	6.169	3.201	4.768	5.482	11.372
+10	-18	6.169	3.201	5.060	5.482	11.372
-10	-18	6.169	3.201	5.644	5.482	11.372
-20	-18	6.169	3.201	5.935	5.482	11.372
-30	-18	6.169	3.201	6.227	5.482	11.372

strange meson σ^* [34] were obtained from the following relations

$$U_{\Xi}^{(\Xi)} \simeq U_{\Lambda}^{(\Xi)} \simeq 2U_{\Xi}^{(\Lambda)} \simeq 2U_{\Lambda}^{(\Lambda)}. \quad (28)$$

The scalar coupling constants are collected in Tables III and IV.

B. The symmetry energy

The TM1 parameter set [6] that successfully describes the ground state properties of both finite nuclei and infinite nuclear matter was supplemented with the mixed nonlinear isoscalar–isovector ω – ρ meson coupling, which provides the additional possibility of modifying the high density components of the symmetry energy. The remaining nuclear matter ground state properties were left unchanged. The symmetry energy is given by the relation

$$E_{sym}(n_b) = \frac{k_F^2}{6\sqrt{k_F^2 + m_{eff,\rho}^2}} + \frac{g_\rho^2}{12\pi^2} \frac{k_F^3}{\hat{m}_{eff,\rho}^2}, \quad (29)$$

where $\hat{m}_{eff,\rho}^2 = m_{eff,\rho}^2 (f_3 = 0)$ denotes the effective mass of the ρ meson in the case of non-strange, symmetric nuclear matter.

The strength of the ω – ρ coupling is set by the $\Lambda_V (g_\omega g_\rho)^2$ and requires the adjustment of the g_ρ coupling constant to keep the empirical value of the symmetry energy $E_{sym}(n_b) = 25.68$ MeV at the baryon density n_b , which corresponds to $k_F = 1.15$ fm $^{-1}$ [19]. The parameters Λ_V together with the adjusted value of the parameter g_ρ are presented in Table V. The density dependence of the symmetry energy can be expressed by coefficients that define the slope L and the curvature K_{sym} of the symmetry energy

$$E_{sym}(n_b) = E_{sym}(n_0) + L \left(\frac{n_b - n_0}{3n_0} \right) + \frac{K_{sym}}{2!} \left(\frac{n_b - n_0}{3n_0} \right)^2. \quad (30)$$

TABLE V. TM1 parameter set with the extended isovector sector [6].

TM1						
$m_\sigma = 511.2$ MeV	$g_\sigma = 10.029$	$g_3 = 7.2325$ fm $^{-1}$				
$m_\omega = 783$ MeV	$g_\omega = 12.614$	$g_4 = 0.6183$				
$m_\rho = 770$ MeV	$g_\rho = 9.264$	$c_3 = 71.0375$				
TM1 nonlinear (isovector sector)						
Λ_V	0	0.014	0.015	0.016	0.0165	0.017
g_ρ	9.264	9.872	9.937	10.003	10.037	10.071
L (MeV)	108.58	77.52	75.81	74.16	73.36	72.56

Equation (30) is a typical low density expansion, higher-order terms must be taken into account at suprasaturation densities. The performed calculations that were focused mainly on the slope parameter of the symmetry energy

$$L = 3n_0 \left. \frac{\partial^2 E_{sym}(n_b)}{\partial n_b^2} \right|_{n_b=n_0} \quad (31)$$

gave results that agreed with the experimental data ($L = 88 \pm 25$ MeV [35]). These results are collected in Table V. However, current estimation of the symmetry energy parameter based on theoretical, experimental and observational results narrows the range of L to (40.5 – 61.9) MeV [36].

V. RESULTS

The energy density and pressure given by relations (24) and (25) define the EoS. Numerical calculations, which were made for the TM1 parameterisation for both non-strange and strangeness-rich matter, led to the solutions that are shown in Fig. 1. A class of EoSs was obtained. Individual EoSs are parametrized by the coupling constant Λ_V , which determines the strength of the mixed vector meson interactions. The form of the EoSs allows one to compare the differences between various models.

An analysis performed for the nonlinear model with parameter Λ_V , which ranges between 0.014 to 0.017, showed that the increase of Λ_V produces a stiffer EoS. For comparison, the EoSs for non-strange matter for NL3, TM1 and FSUGold parameterisations have been included. Thus, the stiffness of the EoS depends on the existence and strength of the mixed vector meson interactions, and the nonlinear model described by the Lagrangian function (6) makes it possible to construct a much stiffer EoS than the one obtained for the TM1-weak model. The abbreviation TM1-weak denotes the standard TM1 model extended to the full octet of baryons with two additional meson fields, which were introduced in a minimal fashion, to reproduce the hyperon–hyperon

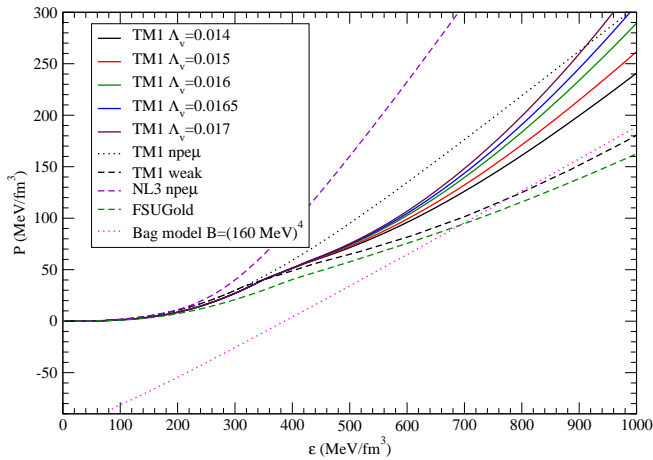


FIG. 1. (Color online) The pressure vs density calculated for selected parameterisations. The stiffest and softest EoS have been obtained for the non-strange matter for NL3 and FSUGold. The EoSs calculated for TM1 parameter set form a distinct class. For these EoSs the stiffest is the one for non-strange matter. It is represented by the dotted line. The nonlinear models for different values of the coupling strength Λ_V are also presented. The upper limit for these models is for $\Lambda_V = 0.017$ the softest represents the case of the standard TM1 model extended by the inclusion of strange mesons which have been introduced in a minimal fashion. The remaining EOS for the nonlinear models with different values of parameter Λ_V are located between these two curves.

interaction. In order to make the analysis more complete, the conditions under which the quark matter occurs in neutron star interiors was established. This permits the formation of a stable hybrid star configuration. Two phases of matter were compared: the strange hadronic matter and the quark matter. The phase with the highest pressure (lowest free energy) was favoured. The dotted curve shows the quark matter EoS for the fixed value of the bag parameter $B^{1/4} = 160$ MeV. The result indicates that there is no intersection of the quark matter EoS and that of hyperon-rich matter calculated for the nonlinear model for a different values of parameter Λ_V , and in this case a hybrid star with a quark phase inside cannot be constructed. Solutions that permit the existence of the quark matter phase inside the hyperon star were obtained for the TM1-weak and FSUGold parameterisations.

In the case of nuclear matter an extended isovector sector comprises the $\omega - \rho$ meson interaction. Parameter Λ_V sets the strength of the $\omega - \rho$ coupling. This term altered the density dependence of the symmetry energy. The standard TM1 parameterisation without $\omega - \rho$ coupling gives as a result very stiff form of the symmetry energy. The inclusion of the $\omega - \rho$ coupling softens the symmetry energy. The solutions were presented in Fig. 2. Calculations were done for rather high value of $\Lambda_V = 0.0165$ and 0.03 . The interaction between ω and ρ mesons leads to the solution, which approaches that obtained for the AV14 and UV14 models with the Urbana

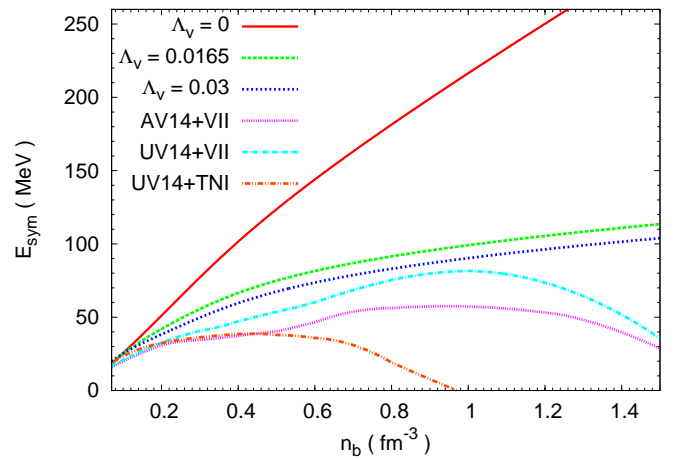


FIG. 2. (Color online) The density dependence of symmetry energy calculated for TM1 parameter set [6] for different values of parameter Λ_V . For comparison the results obtained for the AV14+VII, UV14+VII and UV14+TNI models [37] are included.

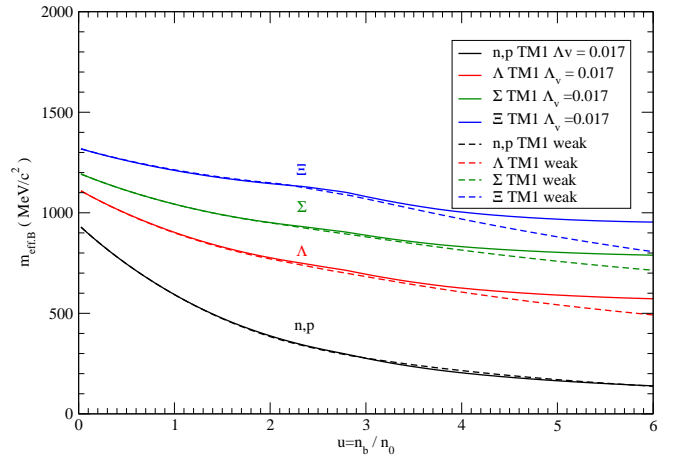


FIG. 3. (Color online) The effective baryon masses as a function of relative baryon density calculated for the nonlinear model, for $\Lambda_V = 0.017$ and for the TM1-weak model.

VII (UV VII) three nucleon potential. For comparison the form of the symmetry energy calculated for the UV14 plus TNI model was included [37].

Interacting baryons are the basic components of the matter of neutron stars. The modification of baryon masses that arises from baryon interactions with the background nuclear matter is shown in Fig. 3. The numerical solutions predicted by equation (18) for the fixed value of parameter $\Lambda_V = 0.017$ for both the nonlinear model and for the TM1-weak model, show reduced effective baryon masses. The reduction of the nucleon mass in the nonlinear model is essentially the same as that obtained in the TM1-weak one. Thus, the influence of the nonlinear vector meson couplings on the nucleon effective mass is negligible. The effective masses of strange baryons in the case of the nonlinear model

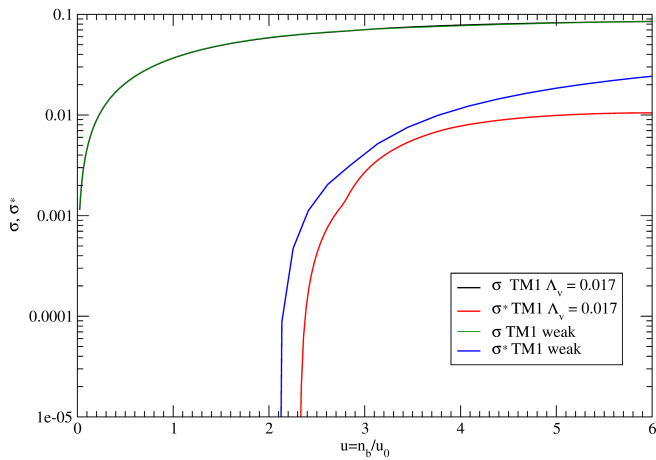


FIG. 4. (Color online) The scalar mesons σ and σ^* as a function of baryon density. For comparison the results obtained for the TM1-weak model have been included.

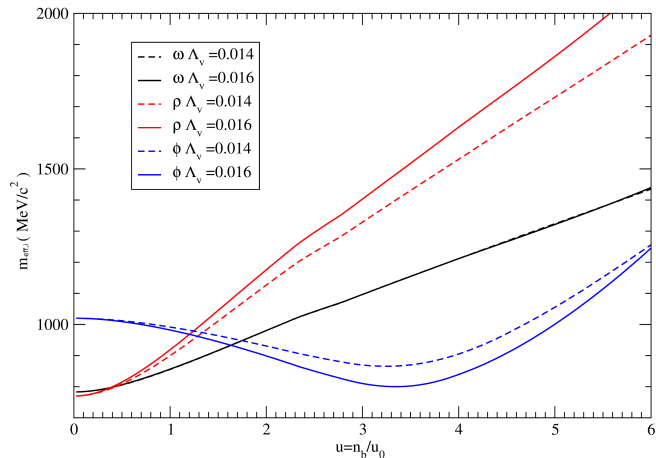


FIG. 5. (Color online) The effective meson masses as a function of baryon number density calculated for the nonlinear model, for $\Lambda_V = 0.014$ and $\Lambda_V = 0.016$.

drop less rapidly than the effective masses obtained in the TM1-weak model. The behaviour of the baryon effective masses is governed by the density dependence of the scalar mean fields, which is presented in Fig. 4. The presence of nonlinear couplings between vector mesons modifies the density dependence of the strange scalar meson leaving the nonstrange scalar meson almost unchanged. The in-medium reduction of baryon masses is equivalent to the modification of vector meson masses in the meson sector (Fig. 5). An analysis of the density dependence of the effective ρ and ϕ vector meson masses led to the conclusion that their modification was produced by a strong Λ_V dependence, especially in the high density limit. The effective mass of the ω meson is almost independent of the value of parameter Λ_V . The stiffness of the EoS is characterised by the incompressibility of nuclear matter. In general, incompressibility comprises terms resulting from the kinetic pressure of Fermi gas and from the po-

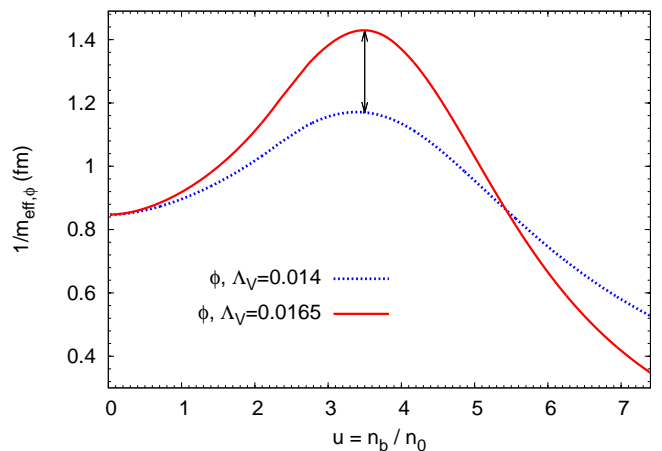


FIG. 6. (Color online) The density dependence of the factor $1/m_{eff,\phi}$ calculated for the nonlinear model, for $\Lambda_V = 0.014$ and $\Lambda_V = 0.0165$.

tential of the model. Analysing the strange sector of the model one can compare the factor that determines the difference between the strength of the effective repulsive and attractive forces. The scalar meson σ^* has been introduced in a minimal fashion thus $m_{eff,\sigma^*} = m_{\sigma^*}$. The strength of the effective repulsive force between strange baryons is mainly altered by the factor $1/m_{eff,\phi}$. The influence of the Λ_V parameter on the density dependence of $1/m_{eff,\phi}$ is depicted in Fig. 6. The increase of the parameter Λ_V considerably enhances the strength of the repulsive force in the system.

The properties of asymmetric strangeness-rich matter of neutron stars are characterized by the parameters that define the strangeness content of the system $f_S = n_S/n_b$, where n_S is the strangeness density and the isospin asymmetry $f_3 = n_3/n_b$, where n_3 is the isospin density given by the relation

$$n_3 = \sum_B I_{3B} n_B \quad (32)$$

The density dependence of the asymmetry parameter and the strangeness content of the system is depicted in Fig. 7. The nonlinear model leads to a system with an enhanced asymmetry and a considerably reduced strangeness. An increase of parameter Λ_V causes the matter to become more asymmetric.

Charge neutrality and the condition of β equilibrium ($p + e^- \leftrightarrow n + \nu_e$) impose constraints on a neutron star composition. Assuming that neutrinos are not considered, since their mean free path is longer than the star radius, the following relation can be obtained

$$\mu_p + \mu_e = \mu_n. \quad (33)$$

Additional hadronic states are produced in neutron star interiors at sufficiently high densities when hyperon in-medium energy equals their chemical potential. The higher the density the more various hadronic species

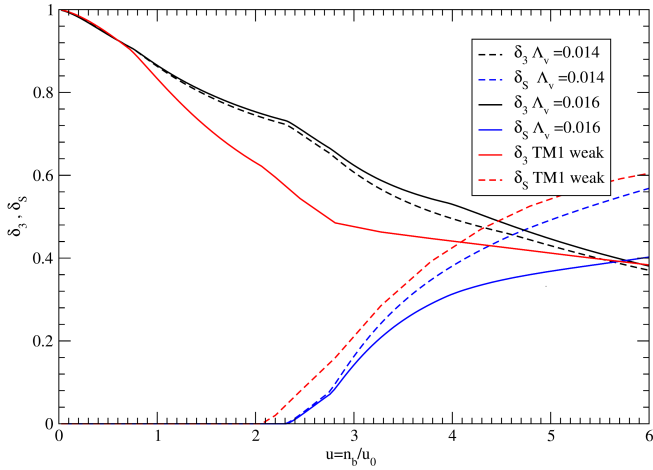


FIG. 7. (Color online) The asymmetry parameters $f_3 = \delta_3$ and $f_S = 3\delta_S$ as a function of baryon number density calculated for the nonlinear model, for different values of Λ_V and for the TM1-weak model.

are expected to populate. In general weak reactions for baryons and the corresponding equations for chemical potentials can be written in the form

$$\begin{aligned} B_1 + l &\leftrightarrow B_2 + \nu_l \\ \mu_B &= b_B \mu_n - q_B \mu_e \end{aligned} \quad (34)$$

where B_1 and B_2 denote baryons, l and ν_l lepton and neutrino of the same flavor, whereas b_B and q_B refer to baryon B with baryon number b_B and charge q_B . The above equations create relations between chemical potentials of particular hyperons

$$\begin{aligned} \mu_\Lambda &= \mu_{\Sigma^0} = \mu_{\Xi^0} = \mu_n; \\ \mu_{\Sigma^-} &= \mu_{\Xi^-} = \mu_n + \mu_e; \\ \mu_p &= \mu_{\Sigma^+} = \mu_n - \mu_e. \end{aligned} \quad (35)$$

The presented equilibrium conditions determine all constituents of the matter of neutron stars. The concentrations of a particular component $i = B, l$ of the matter of a neutron star can be defined as $Y_i = n_i/n_b$, where n_i denotes the density of the component i and n_b is the total baryon number density. The density fraction of nucleons and leptons as a function of the baryon number density for the fixed value of parameter Λ_V is presented in Fig. 8. The important findings concern the concentration of leptons, which are more highly populated in the case of the nonlinear model. Fig. 9 shows how the modification of the vector meson sector alters concentrations of strange baryons. The first hyperon that appears is Λ and it is followed by Ξ^- and Σ^- . The appearance of negatively charged hyperons reduce the concentrations of leptons. This stems from the charge neutrality condition. However, the initial rapid increase in population of Ξ^- hyperons has been suppressed leading to significantly reduced concentration of Ξ^- hyperons at sufficiently high density. For comparison the results obtained for the TM1-weak

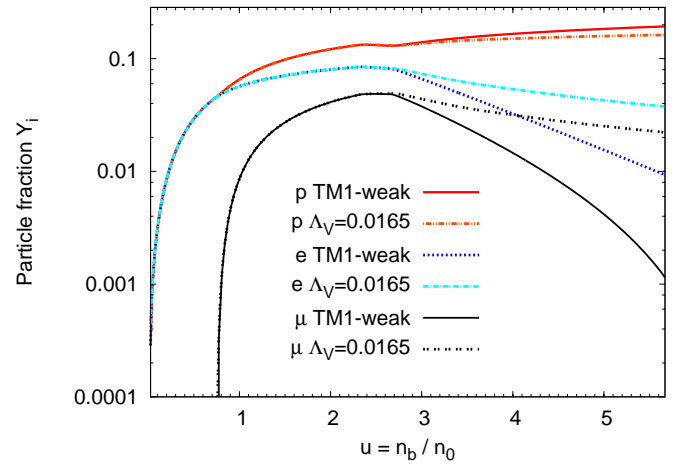


FIG. 8. (Color online) Relative concentrations of nucleons and leptons calculated for the nonlinear model, for the fixed value of parameter $\Lambda_V = 0.0165$. For comparison the results obtained for the TM1-weak model has been included.

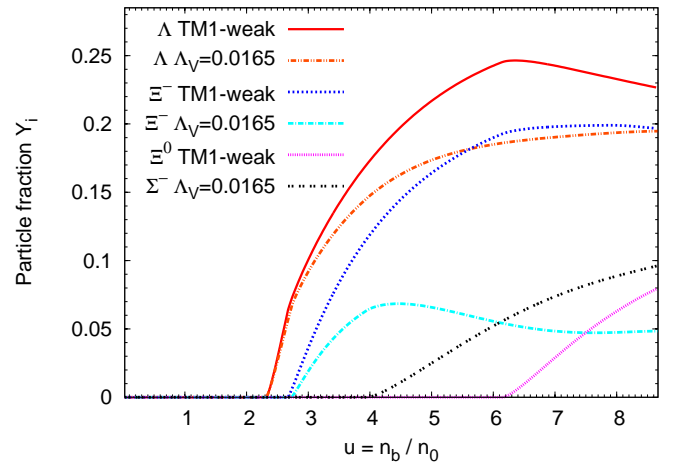


FIG. 9. (Color online) Relative concentrations of strange baryons calculated for the nonlinear model, for the fixed value of parameter $\Lambda_V = 0.0165$. For comparison the results obtained for the TM1-weak model has been included.

model have been included. It is evident that the additional nonlinear couplings between vector mesons modify chemical composition of the neutron star shifting the onset point to higher densities and reduces the strangeness content of the system. A composition and concentrations of hyperons calculated in the nonlinear model can be traced in a chosen configuration of a neutron star. The composition of the core of the maximum mass configuration is depicted in Fig. 10. The number density of Ξ^- hyperons is reduced. However, an interesting feature of this model is the abundance of Σ^- hyperons in the very inner part of the neutron star inner core.

The most essential feature of the model is connected with the fact that even in the presence of hyperons the obtained EoS is very stiff. Global neutron star parameters such as the mass and radius and the structure of a

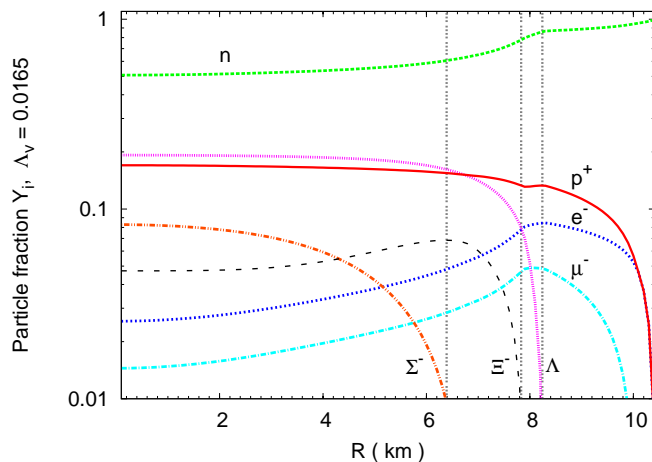


FIG. 10. (Color online) The particle fraction Y_i as a function of the radius of the neutron star, for the maximal mass configuration. Calculations have been done on the basis of nonlinear model with $\Lambda_V = 0.0165$. The dotted vertical lines point the threshold densities for particular hyperons.

neutron star can be determined by the equation of hydrostatic equilibrium - the Tolman-Oppenheimer-Volkoff (TOV) equation:

$$\frac{d\mathcal{P}(r)}{dr} = \frac{-G(\mathcal{E}(r) + \mathcal{P}(r))(m(r) + 4\pi r^3 \mathcal{P}(r))}{r^2 \left(1 - \frac{2Gm(r)}{r}\right)} \quad (36)$$

$$\frac{dm(r)}{dr} = 4\pi r^2 \mathcal{E}(r)$$

$$\frac{dn(r)}{dr} = 4\pi r^2 \left(1 - \frac{2Gm(r)}{r}\right)^{-1/2}$$

where m and n denote the enclosed gravitational mass and baryon number, respectively, \mathcal{P} is the pressure and \mathcal{E} is the total energy density. In order to get the numerical solution of equation (36), the EoS has to be specified. A correct model of a neutron star is based on the assumption that its internal structure is composed of separate parts, thus the construction of the mass-radius relation requires taking into account additional EoSs that describe the matter of the inner and outer crust. For the outer and inner crusts the EoSs of Baym, Pethick, and Sutherland (BPS) [38] and Baym, Bethe and Pethick (BBP) [39] have been used respectively. The results obtained for the set of EoSs calculated in this paper led to the mass-radius relations and permitted the value of the maximum mass to be determined which in a sense can give a measure of the impact of particular nonlinear couplings between vector mesons. In the mass-radius relations obtained for varying values of parameter Λ_V are shown in Fig. 11. The higher the value of Λ_V , the higher the maximum mass.

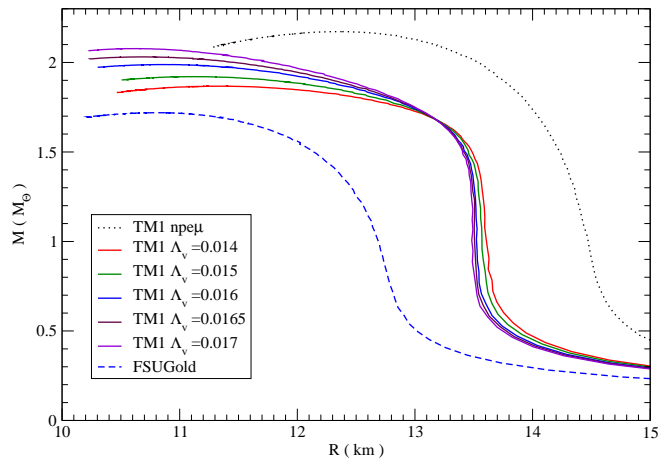


FIG. 11. (Color online) The mass-radius relations calculated for the nonlinear model for different values of parameter Λ_V . The results obtained for both the TM1 parameterisation in the case when the matter of the neutron star comprises only nucleons and for FSUGold parameter set.

VI. THE INFLUENCE OF THE $U_Y^{(N)}$ POTENTIALS

There are still significant uncertainties associated with the experimental data on the hyperon-nucleus interactions. Thus it is reasonable to investigate the effect of the hyperon-nucleus potential $U_Y^{(N)}$ on the obtained results [40]. Particular attention was paid to the dependence of the EoS on the Σ -nucleus potential $U_Y^{(\Sigma)}$. Detailed calculations were done for the selected values of the $U_\Sigma^{(N)}$ potential, assuming its both attractive and repulsive character. Calculations performed for the extended nonlinear model were resulted in a sequence of EoSs (Fig. 12). The stiffest one was obtained for the repulsive potential ($U_\Sigma^{(N)} = 30$ MeV). In order to study the influence of the $U_\Lambda^{(\Lambda)}$ potential a model with an exaggerated value of the potential $U_\Lambda^{(\Lambda)} = 1$ MeV was examined. The resulting change in the EoS is negligible. A similar conclusion can be drawn by examining the changes caused by the reduction in the potential $U_\Xi^{(N)}$. Taking into account the value of the maximum mass obtained for a given EoS the presented results support the conclusion that the value of the potential is not a factor that decisively influences the form of the EoS. A similar conclusion can be obtained by analysing the mass-radius relation (Fig. 13). The most promising results were obtained for the repulsive $U_\Sigma^{(N)} = -30$ MeV potential which within the considered model leads to the highest value of the maximum mass. Hyperons are distributed in the very inner part of a neutron star core therefore a schematic cross-section shows a hyperon core in the inside of a strangeness-rich neutron star. Information concerning properties of the internal structure of a neutron star are summarised in Fig. 14 and 15. These figures depicts the dependence of both

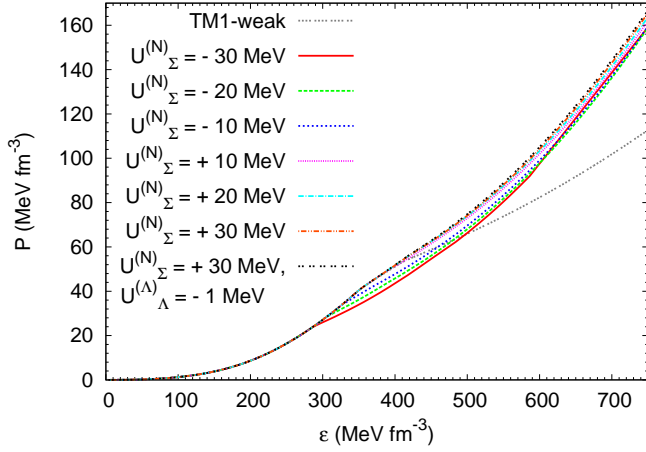


FIG. 12. (Color online) The pressure vs density calculated for different values of the $U_{\Sigma}^{(N)}$ potential (attractive and repulsive), the case of a very weak $\Lambda - \Lambda$ interaction ($U_{\Lambda}^{(\Lambda)} = 1$ MeV) has been also included. For comparison the EoS calculated for the model TM1-weak has been shown.

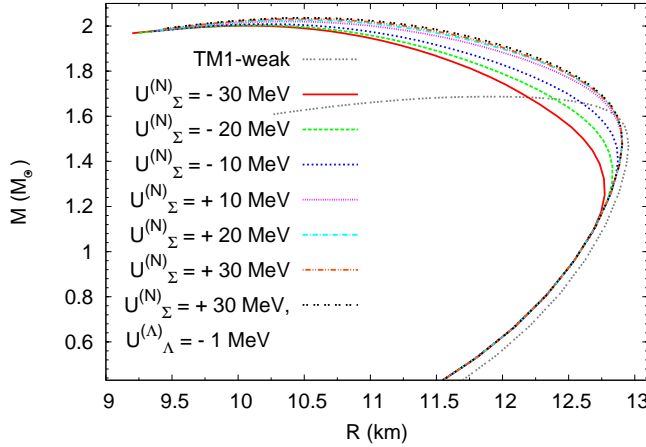


FIG. 13. (Color online) The mass – radius relations calculated for EoSs presented in Fig.12.

neutron stars and their hyperon cores on the $U_{\Sigma}^{(N)}$ potential and strictly speaking on the value of $x_{\Sigma\sigma}$ parameter and offer indications for interpreting the results of numerical calculations. Calculations were done for maximum mass configurations. The mass of the star increases when $U_{\Sigma}^{(N)}$ potential becomes more repulsive whereas the mass of the hyperon core decreases reaching a minimum value for the parameter $x_{\Sigma\sigma} \sim 0.51$ (Fig. 14). Similar behaviour has a radius of the maximum mass configuration. Results are presented in Fig.15. One of the most important difference between the model constructed for the attractive $U_{\Sigma}^{(N)} = -30$ MeV potential and the one with the repulsive potential ($U_{\Sigma}^{(N)} = 30$ MeV) is related to the chemical composition of the neutron star matter. The hyperon onset points depend on the character of the $U_{\Sigma}^{(N)}$ potential. Calculations performed on the basis of

TABLE VI. Neutron star maximum masses and corresponding radii calculated for the chosen values of the potentials $U_{\Sigma}^{(N)}$ and $U_{\Lambda}^{(\Lambda)}$. M_{hc} and R_{hc} denote the mass and radius of a hyperon core for a given maximum mass configuration, $n_{b,onset}$ denotes the hyperon onset point.

$U_{\Sigma}^{(N)}$ (MeV)	$U_{\Lambda}^{(\Lambda)}$ (MeV)	M_s (M_{\odot})	R_s (km)	M_{hc} (M_{\odot})	R_{hc} (km)	$n_{b,onset}$ (fm^{-3})
+30	-1	2.036	10.47	1.620	8.32	0.348
+30	-5	2.032	10.45	1.617	8.31	0.348
+20	-5	2.027	10.44	1.613	8.29	0.348
+10	-5	2.020	10.31	1.609	8.27	0.348
-10	-5	2.008	10.23	1.679	8.38	0.325
-20	-5	2.003	10.18	1.720	8.51	0.305
-30	-5	2.001	10.04	1.768	8.59	0.288

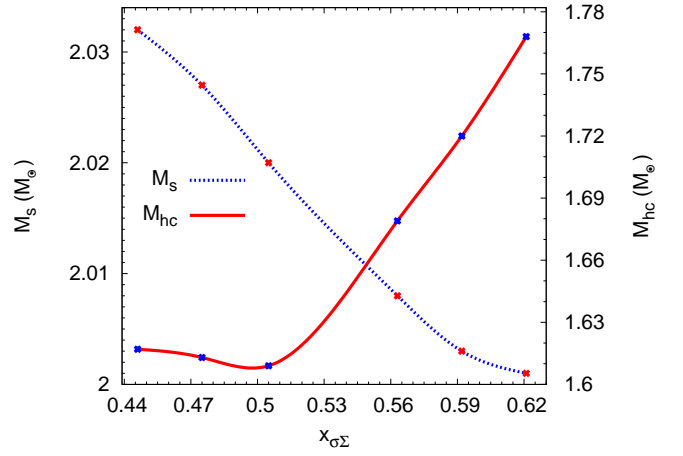


FIG. 14. (Color online) The dotted line shows the dependence of the maximum mass M_s obtained for the given EoS on the value of parameter $x_{\Sigma\sigma}$ that expresses the dependence on the potential $U_{\Sigma}^{(N)}$. Solid line presented similar relations for the mass of the hyperon core M_{hc} .

the extended nonlinear model indicate that reduction of the attractive $U_{\Sigma}^{(N)}$ potential shifts the hyperon onset points to lower densities, whereas the change of the repulsive potential leaves the hyperon onset points almost unchanged (Fig. 16). In the case of attractive potential the first hyperons that appear in neutron star matter are Σ^- hyperons and they are followed by Λ hyperons. Such a scheme of the emergence of hyperons is changed in the nonlinear model with the repulsive $U_{\Sigma}^{(N)} = -30$ MeV potential. The first hyperons that appear are Λ hyperons and successively Ξ^- and Σ^- hyperons. The relative concentrations of hyperons calculated for both attractive and repulsive $U_{\Sigma}^{(N)}$ potential are presented in Fig. 17. The results of numerical calculations obtained for different values of the potential $U_{\Sigma}^{(N)}$ were compiled in Table VI. These results for a given EoS include the value of the maximum mass, the radius of the maximum mass configuration, the radius and mass of the hyperon core and the onset point of hyperons. For comparison the model

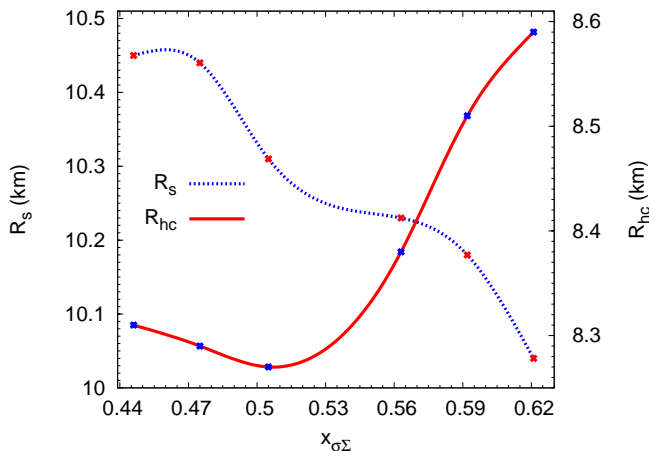


FIG. 15. (Color online) The dotted line shows the dependence of the radius of the maximum mass configurations R_S obtained for the given EoS on the value of parameter $x_{\Sigma\sigma}$ that expresses the dependence on the potential $U_{\Sigma}^{(N)}$. Solid line presented similar relations for the radius of the hyperon core R_{hc}

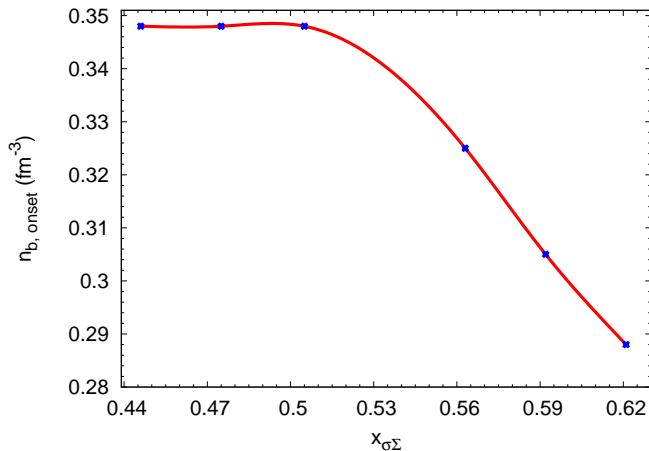


FIG. 16. (Color online) The dependence of the hyperon onset points on the value of the parameter $x_{\Sigma\sigma}$.

with the $U_{\Lambda}^{(\Lambda)} = 1$ MeV was included.

VII. CONCLUSIONS

Recent observations of the binary millisecond pulsars give the value of neutron star mass about two solar masses. In general, theoretical models that describe strangeness-rich neutron star matter lead to much softer EoSs than those constructed for a core of a neutron star composed of only nucleons. This significant softening of the EoS causes a reduction in the maximum mass achievable in a given theoretical model. This leads to an inconsistency between the theoretical models that involve hyperons and the observation. The solution to this problem, is the construction of a theoretical model of the mat-

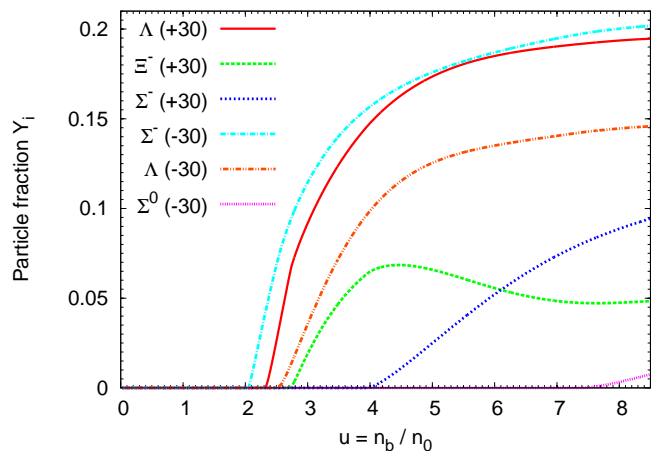


FIG. 17. (Color online) Comparison of the relative concentrations of hyperons calculated for the extended nonlinear model for the repulsive and attractive $U_{\Sigma}^{(N)}$ potential.

ter of a neutron star with hyperons that will give a high value of the maximum mass that demands a stronger repulsive force in the strange sector of the system. The main issue that was addressed in this paper concerns the influence of the nonlinear ω , ρ and ϕ vector mesons on the properties of asymmetric nuclear matter with a non-zero strangeness and consequently on the neutron star parameters. A description of neutron star matter given in this paper was done on the basis of a model inspired by the nonlinear realization of the chiral symmetry. Detailed analysis based on $SU(6)$ and $SU(3)$ symmetry of the behavior of the EoS for different relativistic models have been already done [41–43]. Whereas the analysis of the EoS of hypernuclear matter within a relativistic density functional theory with density-dependent couplings has been included in [44]. An essential aspect of this model is the diverse vector meson sector which comprises different vector meson couplings. As a result, a special class of EoSs adequate to characterise asymmetric nuclear matter with a non-zero strangeness was obtained. Particular EoSs are characterised by the value of parameter Λ_V , which determines the strength of the vector meson couplings. This very special form of the considered model gives an EoS that is much stiffer than that obtained using the standard TM1-weak model. Numerical solutions permitted the influence of the nonlinear vector meson couplings on the density dependence of the scalar and vector meson fields to be investigated. This directly translates to the in-medium properties of baryons and mesons and leads to a considerable modification of the effective baryon and vector meson masses, especially in the strange sector of the model.

The nonlinear vector meson couplings modify both the asymmetry and strangeness content of the system and therefore lead to a model with a reduced strangeness and an enhanced asymmetry. The stiffness of the EoS is directly related to the in-medium properties of the matter

of a neutron star. It depends on value of the effective baryon and meson masses, which modify the compressibility of the matter of a neutron star and the range of interactions especially in the strange sector. The results of the analysis performed in the framework of the nonlinear model have shown that the properties of neutron stars are significantly altered by the presence of hyperons.

The analysis of the dependence of neutron star parameters on the strength of hyperon-nucleon interaction has been already done by Weissenborn et al. [40]. In this paper similar analysis has been performed and in this case the change of the value of hyperon-nucleon potential only slightly modifies the maximum mass of a neutron star, preferring a repulsive character of this potential. However, the changes of the hyperon-nucleon potential influence the parameters of the hyperon core of the neutron star.

The inclusion of hyperons does not soften the EoS; on the contrary, it leads to its considerable stiffening. The consequences for the parameters of neutron stars are

straightforward and appear as the considerable growth of neutron star masses.

In general, the hyperon fraction is reduced in comparison to the linear models. The reduction of the hyperon population in the matter of a neutron star is related to the enhanced lepton concentrations. As an example the maximum mass configuration is presented. In this particular model the core of a neutron star reveal a hyperon inner core with the reduced Λ and Ξ^- hyperon concentrations but with the enhanced population of Σ^- hyperons.

ACKNOWLEDGMENTS

M. Pienkos would like to acknowledge a scholarship from the SWIDER project co-finance by the European Social Fund.

-
- [1] I. Bednarek and M. Pienkos, *Acta Phys. Pol. B* **42**, 2211 (2011).
 - [2] I. Bednarek, *Acta Phys. Pol. B* **140**, 3071 (2009).
 - [3] J. D. Walecka, *Theoretical Nuclear and Subnuclear Physics* (World Scientific, Singapore, 2004).
 - [4] J. Boguta and A. R. Bodmer, *Nucl. Phys. A* **292**, 413 (1977).
 - [5] A. R. Bodmer and C. E. Price, *Nucl. Phys., A* **505**, 123 (1989).
 - [6] Y. Sugahara and H. Toki, *Prog. Theor. Phys.* **92**, 803 (1994).
 - [7] J. Piekarewicz and M. Centelles, *Phys. Rev. C* **79**, 054311 (2009).
 - [8] R. J. Furnstahl, B. D. Serot, and H. B. Tsang, *Nucl. Phys., A* **598**, 539 (1996).
 - [9] R. J. Furnstahl, B. D. Serot, and H. B. Tsang, *Nucl. Phys., A* **615**, 441 (1997).
 - [10] R. Manka and I. Bednarek, *J. Phys. G* **27**, 1975 (2001).
 - [11] J. Carriere, C. J. Horowitz, and J. Piekarewicz, *Astrophys. J.* **593**, 463 (2003).
 - [12] S. K. Singh, M. Bhuyan, P. Panda, and S. K. Patra, *J. Phys. G* **40**, 085104 (2013).
 - [13] B. Todd-Rutel and J. Piekarewicz, *Phys. Rev. Lett.* **95**, 122501 (2005).
 - [14] I. Bednarek, P. Haensel, J. L. Zdunik, M. Bejger, and R. Manka, *A&A* **543**, A157 (2012).
 - [15] P. Demorest, T. Pennucci, S. Ransom, M. Roberts, and J. Hessels, *Nature* **467**, 1081 (2010).
 - [16] J. Antoniadis *et al.*, *Science* **340**, 6131 (2013).
 - [17] P. Papazoglou, S. Schramm, J. Schaffner-Bielich, H. Stoecker, and W. Greiner, *Phys. Rev. C* **57**, 2576 (1998).
 - [18] P. Papazoglou, D. Zschesche, S. Schramm, J. Schaffner-Bielich, H. Stoecker, and W. Greiner, *Phys. Rev. C* **59**, 411 (1999).
 - [19] C. J. Horowitz and J. Piekarewicz, *Phys. Rev. Lett.* **86**, 5647 (2001).
 - [20] G. A. Lalazissis, J. Koenig, and P. Ring, *Phys. Rev. C* **55**, 540 (1997).
 - [21] H. Toki, D. Hirata, Y. Sugahara, K. Sumiyoshi, and I. Tanihata, *Nucl. Phys. A* **588**, c357 (1995).
 - [22] M. Del Estal, M. Centelles, X. Vinas, and S. K. Patra, *Phys. Rev. C* **63**, 024314 (2001).
 - [23] Y. Sugahara and H. Toki, *Nucl. Phys. A* **579**, 557 (1994).
 - [24] T. Hasegawa *et al.*, *Phys. Rev. C* **53**, 1210 (1996).
 - [25] H. Hotchi *et al.*, *Phys. Rev. C* **64**, 044302 (2001).
 - [26] C. B. Dover and A. Gal, *Annals Phys.* **146**, 309 (1983).
 - [27] M. M. Nagels, T. A. Rijken, and J. J. de Swart, *Phys. Rev. D* **15**, 2547 (1975).
 - [28] P. Khaustov *et al.*, *Phys. Rev. C* **61**, 054603 (2000).
 - [29] T. Fukuda *et al.*, *Phys. Rev. C* **58**, 1306 (1998).
 - [30] H. Nouri *et al.*, *Phys. Rev. Lett.* **89**, 072301 (2002).
 - [31] T. Nagae *et al.*, *Phys. Rev. Lett.* **80**, 1605 (1998).
 - [32] H. Takahashi *et al.*, *Phys. Rev. Lett.* **87**, 212502 (2001).
 - [33] I. Bednarek and R. Manka, *J. Phys. G* **36**, 095201 (2009).
 - [34] J. Schaffner and I. N. Mishustin, *Phys. Rev. C* **53**, 1416 (2013).
 - [35] B. K. Agrawal, *Phys. Rev. C* **81**, 034323 (2010).
 - [36] J. M. Lattimer and Y. Lim, *Astrophys. J.* **771**, 51 (2013).
 - [37] R. B. Wiringa and V. Fiks, *Phys. Rev. C* **38**, 1010 (1988).
 - [38] G. Baym, C. Pethick, and P. Sutherland, *Astrophys. J.* **70**, 299 (1971).
 - [39] G. Baym, H. A. Bethe, and C. Pethick, *Nucl. Phys.* **A175**, 225 (1971).
 - [40] S. Weissenborn, D. Chatterjee, and J. Schaffner-Bielich, *Nucl. Phys.* **A881**, 62 (2012).
 - [41] S. Weissenborn, D. Chatterjee, and J. Schaffner-Bielich, *Phys. Rev. C* **85**, 065802 (2012).
 - [42] S. Weissenborn, D. Chatterjee, and J. Schaffner-Bielich, *Nucl. Phys.* **A914**, 421 (2013).
 - [43] T. Miyatsu, M. Cheoun, and K. Saito, *Phys. Rev. C* **88**, 015802 (2013).
 - [44] G. Colucci and A. Sedrakian, *Phys. Rev. C* **87**, 055806 (2013).